

Symmetry-Controlled Thermal Activation in Pyramidal Coulomb Clusters: Testing Kramers-Langer Theory

Akhil Ayyadevara¹, Anand Prakash¹, Shovan Dutta¹, Arun Paramekanti², and S. A. Rangwala¹

¹*Raman Research Institute, C. V. Raman Avenue, Sadashivanagar, Bangalore 560080, India*

²*Department of Physics, University of Toronto, 60 St. George Street, Toronto, Ontario, M5S 1A7 Canada*

(Received 14 January 2026; revised 10 April 2026; accepted 28 May 2026; published 7 July 2026)

Laser-cooled ions confined in electromagnetic traps provide a unique, tunable mesoscopic system where the interplay of the trapping potential, nonlinear Coulomb interactions, and laser-ion scattering generates rich, collective dynamics. In this work, we engineer thermally activated switching between two oppositely oriented, square-pyramidal configurations of five laser-cooled ions in a Paul trap. For identical ions ($^{40}\text{Ca}^+$), the inversions proceed via a *Berry pseudorotation* mechanism with a low activation barrier, enabled by the permutation symmetry, in contrast to the *umbrella inversion* observed in ammonia. The inversion rates obtained from experiments and the Langevin dynamics simulations are accurately captured by the multidimensional Kramers-Langer theory, enabling thermometry of the Doppler-cooled ion cluster at 1.86 ± 0.03 mK. By substituting the apex ion with a heavier isotope ($^{44}\text{Ca}^+$), we break the permutation symmetry and observe a suppression of thermally activated inversions. Numerical analysis reveals that this symmetry breaking closes the low-barrier channel, forcing the system to invert through a high-barrier *turnstile rotation*. Thus, we demonstrate a structural analog of molecular kinetic isotope effects, establishing trapped ions as a versatile platform to explore symmetry-controlled collective dynamics.

DOI: [10.1103/xsxn-srjd](https://doi.org/10.1103/xsxn-srjd)

Rare events—processes that manifest on timescales far exceeding a system’s intrinsic dynamics—are observed in diverse physical settings ranging from protein folding and chemical reactions to nucleation and phase transitions. In thermal equilibrium, these events arise when inherent thermal noise drives the system out of a metastable state. A central theme in statistical mechanics is to develop a predictive, system-independent theory for these kinetics [1]. Kramers provided a foundational framework [2,3] by modeling such transitions as resulting from a Brownian motion in one dimension (1D). Pioneering experiments with single particles in optical traps [4] and levitated nanoparticles [5] have provided remarkable, parameter-free verifications of Kramers’s theory based on real-time tracking [6] and effective 1D reaction coordinates [7,8]. However, complex many-body processes like protein folding, molecular isomerization, and nuclear fission occur in multidimensional energy landscapes, described by the generalized Kramers-Langer (K-L) formalism [9]. Testing this multidimensional framework requires a mesoscopic system close to thermal equilibrium with a complex and controllable energy landscape.

Here, we demonstrate that self-organized Coulomb clusters of laser-cooled trapped ions provide an ideal platform for this purpose. By tuning the anisotropy of the confinement, such a cluster can be steered into a configurational bistability [10,11]. The Doppler-cooling lasers provide an effective thermal bath [12–14], inducing stochastic photon kicks that can activate the transitions,

which can be tracked in real time by measuring the scattered photons. Crucially, as the ions are strongly coupled, local kicks are immediately transferred to all of the ions via collective vibrational modes. Moreover, due to a precise knowledge of the many-body Hamiltonian, these modes and the resulting transition rates from K-L theory can be computed accurately [10,15–17].

We experimentally realize the inversion dynamics of a square-pyramidal cluster of five $^{40}\text{Ca}^+$ ions [Fig. 1(a)]. While geometrically analogous to pyramidal molecules like ammonia, the transition pathway of this Coulomb system reveals a richer structural rearrangement. In particular, we demonstrate how the permutation symmetry of identical ions opens a low-energy pathway, allowing the system to circumvent the high activation barrier of the canonical umbrella inversion. We harness the tunability of the energy barrier to conduct a parameter-free test of the multidimensional K-L theory against Langevin dynamics simulations and apply it to our experimental data to extract the precise thermodynamic temperature of the ion cluster. Furthermore, we test the importance of permutation symmetry in the experiment by substituting the apex with a heavier isotope ($^{44}\text{Ca}^+$), which turns off the low-energy channel, resulting in a directly observable suppression of the inversions.

Pyramidal bistability—We trap and laser cool Ca^+ ions in an end-cap type radio-frequency (*rf*) trap as detailed in our previous studies [10,18,19]. The ions experience a time-averaged harmonic confinement with an angular frequency ω_z along the axial direction and degenerate

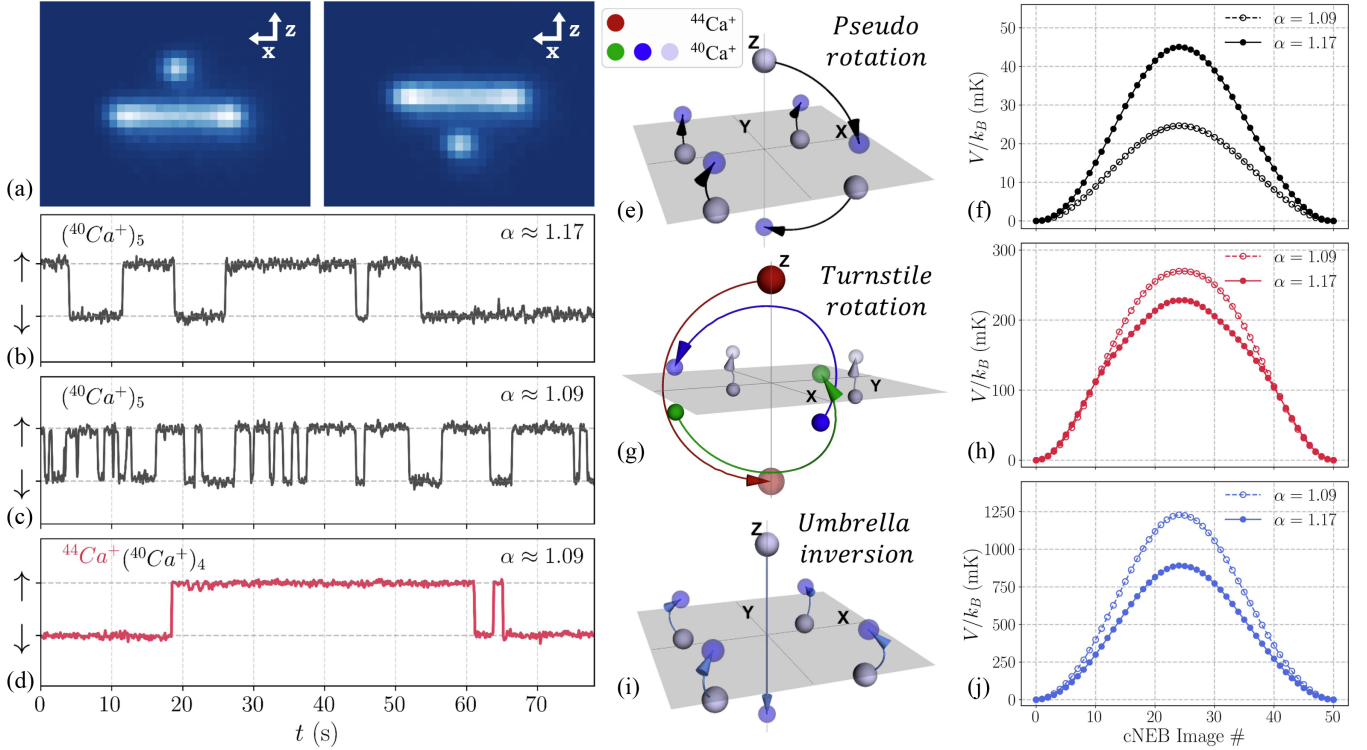


FIG. 1. Inversion mechanisms for a pyramidal ion cluster. (a) Fluorescence images of the two symmetry-broken pyramidal configurations. (b), (c) Experimental time traces of the parity-odd octupole moment $\psi_{3,0}$, showing inversions for an identical-ion cluster at two different settings for the trap aspect ratio α . (d) Suppression of thermal activation after the apex ion is replaced by a heavier isotope. The rare transitions are triggered by background gas collisions. (e), (f) Inversion pathway for the identical cluster is a low-barrier *pseudorotation*. (g), (h) For the isotope-substituted cluster, the rate-limiting path is a *turnstile rotation* with a much higher activation barrier. (i), (j) The canonical *umbrella inversion* involves enormous energy barriers.

angular frequencies $\omega_x = \omega_y$ along the transverse directions due to the cylindrical symmetry of the trap. By superimposing a dc voltage onto the electrodes, we can continuously change the aspect ratio of the confinement, $\alpha = \omega_z/\omega_x$; see Supplemental Material (SM) [20]. The potential energy of five identical ions of mass m is given by

$$V = \sum_{i=1}^5 \left[\frac{m\omega_x^2}{2} (x_i^2 + y_i^2 + \alpha^2 z_i^2) + \sum_{j>i}^5 \frac{k_e e^2}{|\mathbf{r}_i - \mathbf{r}_j|} \right], \quad (1)$$

where $\mathbf{r}_i \equiv (x_i, y_i, z_i)$ are the positions of the ions, e is the electron charge, and k_e is the Coulomb constant.

For $1.05 < \alpha < 1.29$, the global minima of V are two sets of inversion-broken square pyramids [10], where the apex ion is at $(0, 0, \pm z_0)$ and the other four ions form a square at a distance of $z_0/4$ below (above) the x - y plane [Fig. 1(a)]. The height z_0 decreases with increasing α . The ions freely rotate about the z -axis, which blurs the orientation of the four base ions in the fluorescence images due to a finite exposure time. Nonetheless, the inversion breaking is clearly distinguished by the sign of the parity-odd octupole moment, $\psi_{30} \equiv \int d^3r \rho_e(\mathbf{r}) Y_{3,0}(\mathbf{r})$, where $\rho_e(\mathbf{r})$ is the charge distribution and $Y_{3,0}$ is a spherical harmonic. As shown in Figs. 1(b) and 1(c), we observe

stochastic switching between the two polarities with a dramatic increase in the rate as α is lowered.

The pseudorotation pathway—To identify the inversion pathway and how it changes with α , we first note that a switch event occurs over a typical timescale of $\approx 10 \mu\text{s}$ [Fig. 2(a)], during which the cluster rotates uniformly by a small angle ϕ about the z -axis. This is confirmed by molecular dynamics (MD) simulations, discussed below [Fig. 2(c)]. Hence, the ions invert along the minimum energy path (MEP) in configuration space that connects two pyramids with opposite polarity whose azimuthal orientations differ by ϕ . To find this path, it suffices to obtain the MEP corresponding to $\phi = 0$ and then superimpose a uniform rotation. Moreover, since the inversion timescale is comparable to the collective normal-mode oscillation periods (100 kHz–2 MHz) and significantly slower than the rf frequency, we can accurately compute this MEP in the time-averaged potential energy landscape by employing the climbing-image nudged elastic band method [21] widely used for chemical reactions (see SM [20] for more details).

Intuitively, one might expect the inversion to proceed via an umbrella inversion, where the apex pushes through the center of the square base [Fig. 1(i)], similar to the case of an ammonia molecule (NH_3) [25]. However, this pathway

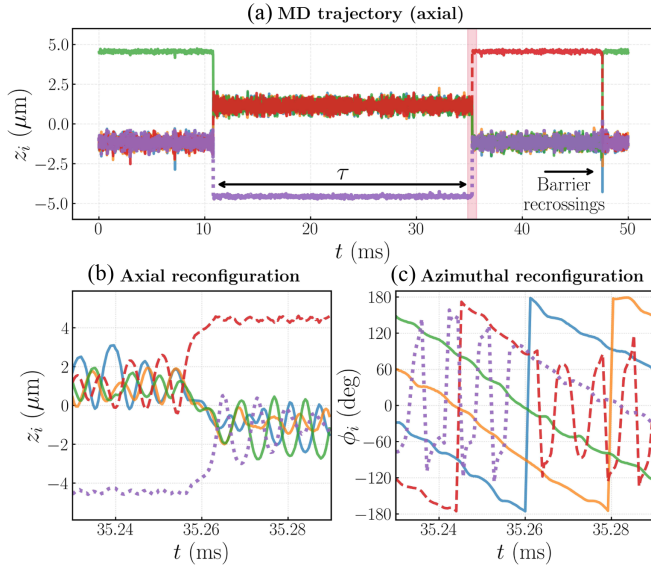


FIG. 2. (a) Trajectory obtained from a MD simulation at an experimentally relevant temperature of 2 mK showing the z -coordinates of five $^{40}\text{Ca}^+$ ions. At the inversion seen at $t \approx 10$ ms, the apex ion (green solid line) moves to the square base, while that base ion (purple dotted line) moves to the inverted apex, completing the pseudorotation. The system remains in this new state for a duration $\tau \approx 25$ ms before inverting back to the initial state, where a different ion (red dashed line) becomes the apex. At $t \approx 48$ ms, we observe rapid barrier recrossings. (b), (c) A closer look at cooperative reconfiguration of all five ions during the inversion at $t \approx 35$ ms, capturing the interchange in the roles of apex ions (purple dotted line and red dashed line) and the nearly uniform rotation of the base ions about the z -axis. The modulations are due to thermal excitation of the collective modes.

incurs a prohibitively high energy cost due to strong Coulomb repulsion at the planar transition state [Fig. 1(j)]. Instead, the cluster finds a significantly lower-energy pathway, whereby the apex ion replaces a base ion, while that base ion moves to the new apex [Fig. 1(e)]. This cooperative exchange is analogous to the pseudorotation mechanism found in certain molecules, where the displacement of only a few atoms results in an effective rotation of the entire molecule [26].

Along this pathway, the ions maintain larger pairwise separations compared to the umbrella inversion, greatly reducing the Coulomb energy cost and lowering the activation barrier by approximately two orders of magnitude [Fig. 1(f)]. In addition, lowering the trap aspect ratio α reduces the activation barrier, since it allows for a larger axial separation z_0 . This explains the higher inversion rate observed at lower α [Figs. 1(b) and 1(c)].

Isotope substitution—The pseudorotation pathway is enabled by the permutation symmetry between the apex and the base ions of the pyramid. Breaking this symmetry has dramatic consequences. Experimentally, we break the permutation symmetry by substituting one ion with a heavier isotope ($^{44}\text{Ca}^+$; next higher in abundance after

$^{40}\text{Ca}^+$ [27]), which preferentially occupies the apex of the pyramid (see SM [20]). The pseudorotation is no longer viable, as it does not invert the pyramid. Instead, the ions have to undergo a cooperative exchange of three ions [Fig. 1(g)] akin to a turnstile rotation [28,29] with much higher energy barriers [Fig. 1(h)].

The suppression of inversion dynamics due to such high energy barriers is strikingly visible in our real-time traces obtained from fluorescence images. Under identical trapping conditions ($\alpha \approx 1.09$), the $(^{40}\text{Ca}^+)_5$ cluster undergoes rapid inversions [Fig. 1(c)], whereas the $^{44}\text{Ca}^+(^{40}\text{Ca}^+)_4$ cluster remains locked in one orientation over long periods [Fig. 1(d)], realizing a structural analog of a giant kinetic isotope effect [30,31]. This observation demonstrates that the rapid inversions indeed occur via the symmetry-enabled pseudorotation.

Testing Kramers-Langer theory—Having confirmed the symmetry-assisted nature of the inversions in the mono-isotopic $(^{40}\text{Ca}^+)_5$ cluster, which can be controlled by tuning the aspect ratio α [Figs. 1(b) and 1(c)], we turn to the test of the multidimensional K-L theory. First, we compare the K-L theory with MD simulations of the microscopic dynamics at different temperatures and trap aspect ratios to examine its validity.

The dynamics of the ions are governed by the interplay of the conservative trap and Coulomb potentials, $V(\{\mathbf{r}_i\})$, and the nonconservative forces from the Doppler cooling lasers. In the experiment, the photon scattering rate ($\Gamma/2\pi \approx 22$ MHz) is much larger than the secular frequencies ($\omega_{x,z}/2\pi \approx 1$ MHz), so the laser interaction can be modeled by a viscous friction force and a stochastic fluctuating force [12–14]. Consequently, the motion of the ions is described by the coupled underdamped Langevin equations [32,33]:

$$m\ddot{\mathbf{r}}_i + \gamma\dot{\mathbf{r}}_i + \nabla_i V(\{\mathbf{r}_j\}) = \boldsymbol{\xi}_i(t). \quad (2)$$

Here, γ is the friction coefficient determined by the laser detuning and intensity [34], and $\boldsymbol{\xi}_i(t)$ represents a Gaussian white noise satisfying the fluctuation-dissipation relation $\langle \xi_{i,\alpha}(t)\xi_{j,\beta}(t') \rangle = 2m\gamma k_B T \delta_{ij}\delta_{\alpha\beta}\delta(t-t')$, where T is the equilibrium temperature.

A typical trajectory obtained from MD simulations of Eq. (2) is shown in Fig. 2, where the pseudorotation mechanism is evident. We extract the inversion rate κ from an exponential distribution of the dwell time τ from more than 2000 trajectories. We also find barrier recrossings with very short dwell times ($\tau \ll m/\gamma$) typically seen in underdamped Brownian dynamics [35,36], which are excluded from the rate calculation (see SM [20]).

On the other hand, the escape rate from a local minimum predicted by the multidimensional K-L theory is [9]

$$\kappa = \mathcal{N} \frac{\lambda^+}{2\pi} \left(\frac{\det \mathbf{U}}{|\det \mathbf{U}'|} \right)^{1/2} \exp(-E_b/k_B T), \quad (3)$$

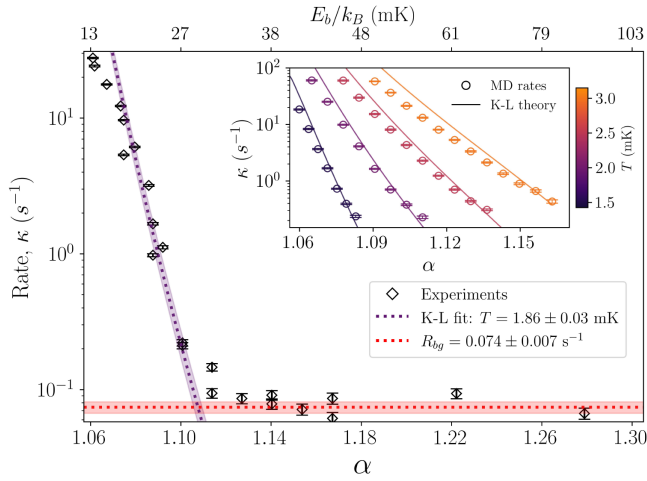


FIG. 3. Experimentally measured pyramidal inversion rates fitted to the K-L theory to determine the cluster temperature T and the inversion rate R_{bg} due to background collisions. (Inset) Agreement between the inversion rates obtained from MD simulations at four different temperatures to the corresponding K-L theory predictions without any fit parameters.

where E_b is the energy barrier and \mathbf{U} , \mathbf{U}' are the Hessian matrices at the equilibrium and saddle points along the MEP, respectively. The prefactor λ^+ is the single positive eigenvalue of the dynamical matrix at the saddle,

$$\det(m\lambda^2\mathbf{I} + \gamma\lambda\mathbf{I} + \mathbf{U}') = 0, \quad (4)$$

which accounts for the curvature along the unstable mode at the saddle point and the damping γ . The additional factor \mathcal{N} denotes the number of equivalent pathways connecting the same initial and final states [3] (see SM [20] for an illustration in a toy model).

Before applying this formula to our cluster, we note that the rotational symmetry about the z -axis results in a zero-frequency Goldstone mode at both the equilibrium and saddle points [10]. This free rotation does not affect the inversion dynamics, and thus, we exclude this mode in the Hessians, as usual [3]. We also set $\mathcal{N} = 4$, since the apex ion can replace any of the four base ions. As shown in the inset of Fig. 3, the rates obtained from MD simulations show excellent parameter-free agreement with the K-L predictions over a wide range of α for temperatures of 1.5–3 mK. The agreement is better at lower temperatures and higher barriers, as expected [3].

The experimentally measured inversion rate, robustly extracted from the autocorrelation of the time traces [20,22], exhibits a clear threshold behavior (Fig. 3). For $\alpha < \alpha_{th} \sim 1.1$, it grows rapidly as the barrier height is lowered, whereas for $\alpha > \alpha_{th}$, it saturates to $R_{bg} = 0.074 \pm 0.007 \text{ s}^{-1}$ due to background gas collisions. Because the multidimensional K-L prefactors and activation barriers are fully determined from our numerical calculations and validated via MD simulations, they establish a fixed,

predictive framework. Consequently, when evaluating the experimental data, the macroscopic temperature in the Arrhenius exponential term is the only free parameter. The excess rate for $\alpha < \alpha_{th}$ matches the analytical K-L prediction over two orders of magnitude for a fitted temperature of $T = 1.86 \pm 0.03 \text{ mK}$. This agreement confirms that the rapid inversions are indeed thermally activated and validates the applicability of the K-L theory to this strongly coupled, mesoscopic system, allowing us to determine its temperature.

Discussion—We have tested the multidimensional K-L theory in a genuine many-body setting. By tuning five identical $^{40}\text{Ca}^+$ ions into a bistable square-pyramidal configuration, we uncover a coordinated exchange of the ions enabled by permutation symmetry akin to pseudorotations observed in molecules rather than the conventional umbrella inversion. The activation barrier can be tuned by varying the trap anisotropy, enabling the experimentally measured inversion rates to span over two decades. The quantitative agreement between our measurements, MD simulations, and the full K-L prediction (up to a small offset due to unavoidable background collisions) not only confirms the theory’s predictive power for collective, high-dimensional escape processes, but also yields an *in situ* cluster temperature of $1.86 \pm 0.03 \text{ mK}$, approaching the Doppler-cooling limit.

As the microscopic inversion mechanism itself cannot be directly observed in the experiment, we verify the critical role of permutation symmetry via isotope substitution. By replacing one $^{40}\text{Ca}^+$ with a heavier $^{44}\text{Ca}^+$, we exploit the mass dependence of the harmonic potential to energetically “pin” the impurity at the apex. The resulting suppression of thermally activated inversions is analogous to a giant kinetic isotope effect in molecular reactions [30,31]. Interestingly, the residual inversions due to background collisions are also much rarer for the isotope-substituted cluster [see Figs. 1(d) and 3], which highlights the subtle interplay between the background collisions and the continuous cooling in the rare inversions of bistable ion clusters [37].

In conclusion, our results present laser-cooled Coulomb clusters as a pristine many-body system for engineering thermally activated dynamics. While we test the Markovian limit of constant Doppler cooling, the effects of different laser cooling protocols [38–40] on the inversion dynamics can be investigated. As an alternative to isotope substitution, one can harness internal electronic states or vibrational quanta as a programmable means of breaking the permutation symmetry [41–43]. This would enable the study of “active” symmetry breaking, where the system is driven to specific reaction pathways by coherently preparing the internal states [44], thereby bridging reaction kinetics and quantum control.

Acknowledgments—We thank Sanjib Sabhapandit and Satya N. Majumdar for fruitful discussions. We

acknowledge support from the Department of Science and Technology and the Ministry of Electronics and Information Technology, Government of India, under the “Centre for Excellence in Quantum Technologies” grant with Ref. No. 4(7)/2020-ITEA. A. Paramekanti acknowledges funding via Discovery Grant No. RGPIN-2026-0457 from the Natural Sciences and Engineering Research Council (NSERC) of Canada.

Data availability—There are no publicly available research data or software supporting this manuscript. Requests for further information or data should be sent to the authors.

-
- [1] B. Peters, *Reaction Rate Theory and Rare Events Simulations* (Elsevier, Amsterdam, 2017).
- [2] H. Kramers, Brownian motion in a field of force and the diffusion model of chemical reactions, *Physica A (Amsterdam)* **7**, 284 (1940).
- [3] P. Hänggi, P. Talkner, and M. Borkovec, Reaction-rate theory: Fifty years after Kramers, *Rev. Mod. Phys.* **62**, 251 (1990).
- [4] L. McCann, M. Dykman, and B. Golding, Thermally activated transitions in a bistable three-dimensional optical trap, *Nature (London)* **402**, 785 (1999).
- [5] L. Rondin *et al.*, Direct measurement of Kramers turnover with a levitated nanoparticle, *Nat. Nanotechnol.* **12**, 1130 (2017).
- [6] T. Li, S. Kheifets, D. Medellin, and M. G. Raizen, Measurement of the instantaneous velocity of a Brownian particle, *Science* **328**, 1673 (2010).
- [7] A. Berezhkovskii and A. Szabo, One-dimensional reaction coordinates for diffusive activated rate processes in many dimensions, *J. Chem. Phys.* **122**, 014503 (2005).
- [8] N. Zijlstra, D. Nettel, R. Satija, D. E. Makarov, and B. Schuler, Transition path dynamics of a dielectric particle in a bistable optical trap, *Phys. Rev. Lett.* **125**, 146001 (2020).
- [9] J. Langer, Statistical theory of the decay of metastable states, *Ann. Phys. (N.Y.)* **54**, 258 (1969).
- [10] A. Ayyadevara, A. Prakash, S. Dutta, A. Paramekanti, and S. A. Rangwala, Observing octupolar charge orders and their transition dynamics in Coulomb clusters, *Phys. Rev. Res.* **8**, L012066 (2026).
- [11] N. Mizukami, G. Gatta, L. Duca, and C. Sias, Emulating isomerization with two-dimensional Coulomb crystals, [arXiv:2508.05902](https://arxiv.org/abs/2508.05902).
- [12] J. Javanainen and S. Stenholm, Laser cooling of trapped particles I: The heavy particle limit, *Appl. Phys.* **21**, 283 (1980).
- [13] J. Javanainen, Light-pressure cooling of a crystal, *Phys. Rev. Lett.* **56**, 1798 (1986).
- [14] G. Morigi and J. Eschner, Doppler cooling of a Coulomb crystal, *Phys. Rev. A* **64**, 063407 (2001).
- [15] H. Landa, M. Drewsen, B. Reznik, and A. Retzker, Modes of oscillation in radiofrequency Paul traps, *New J. Phys.* **14**, 093023 (2012).
- [16] H. Kaufmann, S. Ulm, G. Jacob, U. Poschinger, H. Landa, A. Retzker, M. B. Plenio, and F. SchmidtKaler, Precise experimental investigation of eigenmodes in a planar ion crystal, *Phys. Rev. Lett.* **109**, 263003 (2012).
- [17] J. Kiethe, L. Timm, H. Landa, D. Kalincev, G. Morigi, and T. E. Mehlstaubler, Finite-temperature spectrum at the symmetry-breaking linear to zigzag transition, *Phys. Rev. B* **103**, 104106 (2021).
- [18] A. Prakash, A. Ayyadevara, E. Krishnakumar, and S. A. Rangwala, Low divergence cold-wall oven for loading ion traps, *Rev. Sci. Instrum.* **95**, 033202 (2024).
- [19] A. Prakash *et al.*, Endcap-type Paul trap for precision spectroscopy and studies of controlled interactions, [arXiv:2601.07328](https://arxiv.org/abs/2601.07328).
- [20] See Supplemental Material at <http://link.aps.org/supplemental/10.1103/xsdn-srjd>, which includes Refs. [10,19,21–24], for description of the experimental system, numerical methods to obtain the K-L prefactors and energy barriers, MD simulations, a toy problem to demonstrate the multiplicity factor in K-L rates under degenerate pathways, and the autocovariance rate estimator for experimental time traces.
- [21] G. Henkelman, B. P. Uberuaga, and H. Jónsson, A climbing image nudged elastic band method for finding saddle points and minimum energy paths, *J. Chem. Phys.* **113**, 9901 (2000).
- [22] D. Chandler, Statistical mechanics of isomerization dynamics in liquids and the transition state approximation, *J. Chem. Phys.* **68**, 2959 (1978).
- [23] C. Schrama, E. Peik, W. Smith, and H. Walther, Novel miniature ion traps, *Opt. Commun.* **101**, 32 (1993).
- [24] N. Grønbech-Jensen and O. Farago, A simple and effective Verlet-type algorithm for simulating Langevin dynamics, *Mol. Phys.* **111**, 983 (2013).
- [25] J. M. Lehn, *Nitrogen inversion*, in *Dynamic Stereochemistry*, Fortschritte der Chemischen Forschung, Vol. 15/3 (Springer, Berlin, Heidelberg, 1970).
- [26] R. S. Berry, Correlation of rates of intramolecular tunneling processes, with application to some group V compounds, *J. Chem. Phys.* **32**, 933 (1960).
- [27] T. Coplen *et al.*, Isotope-abundance variations of selected elements (IUPAC technical report), *Pure Appl. Chem.* **74**, 1987 (2002).
- [28] S. Matsukawa, H. Yamamichi, Y. Yamamoto, and K. Ando, Pentacoordinate organoantimony compounds that isomerize by turnstile rotation, *J. Am. Chem. Soc.* **131**, 3418 (2009).
- [29] E. P. A. Couzijn, J. C. Slootweg, A. W. Ehlers, and K. Lammertsma, Stereomutation of pentavalent compounds: Validating the Berry pseudorotation, redressing Ugi’s turnstile rotation, and revealing the two- and three-arm turnstiles, *J. Am. Chem. Soc.* **132**, 18127 (2010).
- [30] Z. Zhao, Z. Zhang, S. Liu *et al.*, Dynamical barrier and isotope effects in the simplest substitution reaction via Walden inversion mechanism, *Nat. Commun.* **8**, 14506 (2017).
- [31] L. S. Petralia *et al.*, Strong inverse kinetic isotope effect observed in ammonia charge exchange reactions, *Nat. Commun.* **11**, 173 (2020).
- [32] S. Ulm *et al.*, Observation of the Kibble–Zurek scaling law for defect formation in ion crystals, *Nat. Commun.* **4**, 2290 (2013).

- [33] K. Pyka *et al.*, Topological defect formation and spontaneous symmetry breaking in ion Coulomb crystals, *Nat. Commun.* **4**, 2291 (2013).
- [34] D. Leibfried, R. Blatt, C. Monroe, and D. Wineland, Quantum dynamics of single trapped ions, *Rev. Mod. Phys.* **75**, 281 (2003).
- [35] A. Lyons, A. Devi, N. Q. Hoffer, and M. T. Woodside, Quantifying the properties of nonproductive attempts at thermally activated energy-barrier crossing through direct observation, *Phys. Rev. X* **14**, 011017 (2024).
- [36] A. M. Berezhkovskii and D. E. Makarov, Barrier recrossing dynamics and phenomenological rate equations from single-molecule perspective, *J. Chem. Phys.* **163**, 051101 (2025).
- [37] G. Pagano *et al.*, Cryogenic trapped-ion system for large scale quantum simulation, *Quantum Sci. Technol.* **4**, 014004 (2018).
- [38] D. Reiß *et al.*, Raman cooling and heating of two trapped Ba⁺ ions, *Phys. Rev. A* **65**, 053401 (2002).
- [39] J. Roßnagel, K. N. Tolazzi, F. Schmidt-Kaler, and K. Singer, Fast thermometry for trapped ions using dark resonances, *New J. Phys.* **17**, 045004 (2015).
- [40] B. de Neeve, T. L. Nguyen, A. Ferk, T. Behrle, F. Lancellotti, M. Simoni, S. Welte, and J. P. Home, Modular variable laser cooling for efficient entropy extraction, *Phys. Rev. Lett.* **134**, 203603 (2025).
- [41] C. Monroe *et al.*, Programmable quantum simulations of spin systems with trapped ions, *Rev. Mod. Phys.* **93**, 025001 (2021).
- [42] M. Mazzanti, R. Gerritsma, R. J. C. Spreeuw, and A. Safavi-Naini, Trapped ions quantum logic gate with optical tweezers and the Magnus effect, *Phys. Rev. Res.* **5**, 033036 (2023).
- [43] Z. Sun, Y. H. Teoh, F. Rajabi, and R. Islam, Two-dimensional ion crystals in a hybrid optical cavity trap for quantum information processing, *Phys. Rev. A* **109**, 032426 (2024).
- [44] M. Mallweger *et al.*, Probing electronic state-dependent conformational changes in a trapped Rydberg ion Wigner crystal, *Phys. Rev. Lett.* (2026)..